Journal of Colloid and Interface Science 711 (2026) 140071

Contents lists available at ScienceDirect

Journal of Colloid And Interface Science

journal homepage: www.elsevier.com/locate/jcis

Non-invasive multiscale characterization of protein networks and oil droplets in emulsions using spin-echo small angle neutron scattering

Eleonora Olsmats [a,*], Adrian R. Rennie [a], Jeroen Plomp [b], Michel Thijs [b], Coen Fransen [b], Chris Duif [b], Wim Bouwman [b]

[a] Macromolecular Chemistry, Department of Chemistry – Ångström, Uppsala University, Box 538, 751 20 Uppsala, Sweden
[b] Faculty of Applied Sciences, Delft University of Technology, Mekelweg 15, Delft 2629, JB, the Netherlands

HIGHLIGHTS

- Pea proteins form hydrated networks at neutral pH, supporting emulsion stability.
- Emulsion droplet size decreases with higher oil fraction but increases at lower pH.
- Protein denaturation at low pH causes aggregation into large clusters.
- SESANS enables real-space study of emulsions and protein dispersions without dilution.
- Contrast variation with D_2O/H_2O separates scattering of protein and the oil.

GRAPHICAL ABSTRACT

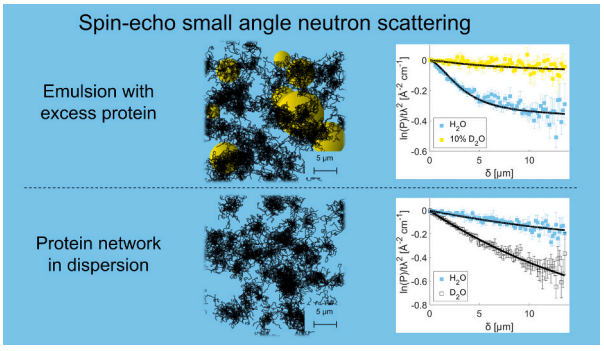

ARTICLE INFO

Dataset link: SESANS, SANS, USAXS & SAXS data sets (Original data)

Keywords:
Pea protein
Emulsion
Protein gel
Fractal network
Spin-echo small angle neutron scattering (SESANS)
Contrast variation

ABSTRACT

Hypothesis: Pea proteins can act not only as interfacial stabilizers of oil-in-water emulsions but also as gelling agents in the continuous phase. Protein gelation, rather than droplet jamming, may be the main mechanism of emulsion stability, providing a physical explanation for the creaminess of high-protein plant-based emulsions.
Experimental: Spin-echo small angle neutron scattering (SESANS) with D_2O/H_2O contrast variation was used to study 15% pea protein dispersions and emulsions with 40–60% rapeseed oil, 7.5% protein at pH 3 to 6.5. SESANS investigates length scales up to tens of micrometres, enabling simultaneous analysis of protein networks and oil droplets without dilution. Complementary small angle X-ray/neutron scattering were used to validate protein aggregate size, and hydration.
Findings: Protein dispersions at neutral pH formed mass fractal networks with small individual building blocks (radius ~38 Å, hydration ~70%). Emulsions consisted of oil droplets embedded in these networks, with droplet radii decreasing at higher oil fractions due to an effective higher protein concentration in the continuous phase, creating a denser network. Dispersions and emulsions at lower pH contained aggregated clusters of denatured proteins. These coarse and inhomogeneous networks gave increasing droplet radii at lower pH. Contrast variation enabled the separation of protein and oil droplet scattering, demonstrating that protein gelation rather than droplet jamming is the main mechanism of stability. This gives a physical explanation of the high viscosity of

* Corresponding author.
E-mail address: Eleonora.Olsmats@kemi.uu.se (E. Olsmats).

https://doi.org/10.1016/j.jcis.2026.140071
Received 3 October 2025; Received in revised form 30 December 2025; Accepted 5 February 2026
Available online 7 February 2026

high-protein plant-based emulsions and is promising for these plant materials to be used as gelling agents in food applications.

1. Introduction

Uses of emulsions range from food materials, pharmaceutical delivery systems and agrochemicals. These occur as industrial products and in the natural environment and people come in contact with them on an everyday basis [1–3]. As a mixture of two immiscible liquids, found only in a kinetically stable state except for microemulsions, the main concern is stability where droplet size changes with time due to flocculation, coalescence or Ostwald ripening that leads eventually to phase separation [4]. Usually there is a third component that adsorbs at the interface between the two liquids and prevents the droplets from contact, thus hindering coalescence. This material can be low-molecular weight surfactants, proteins that are amphiphilic in nature, or solid particles forming so-called Pickering emulsions [5,6]. Pickering particles and large protein aggregates at the interface have potential particularly in the food industry as they can be made from sustainable materials that are healthy to consume. Additionally, a major advantage with the use of large particles and macromolecules as stabilizers is the high desorption energy required to detach the material from the interface. This effectively makes the emulsions irreversibly stable, resembling the properties of thermodynamically stable microemulsions. Our previous studies of phase separated emulsions stabilized by pea proteins have identified a reproducible composition that resembles equilibrium stability [7]. It was found that there is gel formation but the structural origin of the gelation was ambiguous. An objective of this study is to determine whether the gelation is due to the simple jamming of droplets or to protein interactions.

While the physical principles of model emulsion systems are simple to understand, materials suitable for food applications often consist of many different components. An example of a promising material for formulations is pea protein isolate, which has been shown to act as stabilizers for a range of different oil fractions and concentrations of stabilizer [8]. Particularly, high-protein emulsions are interesting from a nutritional perspective. In such emulsions, sometimes referred to as emulsion gels, a substantial amount of protein is located in the continuous phase as a viscosity enhancer to mimic creaminess of products with higher saturated fat content. Despite the promising use of pea and other types of vegetable protein materials as both emulsion stabilizers and gelling agents, little is known about the combined mechanisms for emulsion gel stability. Results of pea protein dispersion and emulsion structures obtained from small angle neutron scattering (SANS) [9], small-angle X-ray scattering (SAXS) [7,9,10], ultra-small angle X-ray scattering (USAXS) [7,10] and confocal microscopy [7,9] have been described. While there is a lot of information gained from these techniques, there are certain limitations in order to resolve the combined structure. SANS is useful to study the structure of individual proteins when different contrasts are used for these multi-component emulsions and protein gels that exploit the differences in scattering cross-sections of isotopes [11], particularly hydrogen and deuterium. Both protein hydration, individual sizes and location can accurately be obtained from such measurements [9]. This has also been shown to be a valuable technique to study liquid foams stabilized by albumins from pea proteins [12]. However, limited information about the larger protein structures forming the gelled networks, aggregates of protein and micrometre sized oil droplets or plateau borders in foams can be deduced. USAXS is able to provide such information about larger structures, however, it is difficult to distinguish between the signals from oil droplets and large protein structures separately due to the fixed scattering length density difference between the components. Confocal microscopy can also observe both oil droplets and protein when labelled with dyes that fluoresce at different wavelengths, but image analysis only covers a limited number of droplets and requires some interpretation with criteria for identification of object boundaries and shapes. Light scattering techniques are also possibilities to determine size distributions, however they are not feasible for these concentrated and opaque samples and would require dilution to make them sufficiently transparent which changes the stability limits in these systems. An account as to how the composition alters the stability has previously been described on the samples in this study [10] and from a survey of other work [8].

This study uses spin-echo SANS (SESANS), a non-invasive technique without the need for sample dilution or manipulation, that takes advantage of the same contrast variation as in SANS experiments, but extends the available size range to cover structures up to several micrometres. It provides directly real-space correlation functions. It complements ultra-SANS (USANS) experiments that would cover similar length scales but with different considerations of resolution and multiple scattering. Both protein structures and oil droplets have dimensions in this range of sizes. SESANS has previously been used to study samples such as dairy products [13,14], capillary suspensions consisting of whey protein particles in oil, where a small amount of water acts as the secondary liquid and forms capillary bridges between the particles [15], emulsion gels with whey proteins [16,17] and ovalbumin gels [18]. However, the use of contrast variation in SESANS has not been fully utilized and the experiments in each of the studies mentioned above have been performed at one contrast only. By varying the ratio of D_2O to H_2O in the aqueous phase, signal from protein and oil can be analysed separately and adds extra novelty to this work. Conventional SANS has previously been performed on emulsions with deuterated oils [19], however, this study shows that SESANS can provide information about droplets and proteins by varying H_2O to D_2O ratio even without using deuterated oils.

The samples investigated in this work include dispersions and emulsions of a plant-based material that would be suitable to use in the food industry. The protein dispersions are prepared with 15% w/v of pea protein isolate in water (pH 6.5) or citrate buffer (pH 3.0 to 6.2). The emulsion samples are prepared with 40–60% v/v rapeseed oil in water or citrate buffer, stabilized with a total of 7.5% w/v of pea proteins.

2. Experimental

2.1. Materials

Pea protein isolate (*Pisum sativum* L.) was obtained from Superfruit Scandinavia AB (Växjö, Sweden), and had a declared protein content of 83% w/w. According to the supplier, the remaining material is 6.8% w/w unsaturated fat, 5.3% w/w carbohydrates as insoluble fibres, water and soluble salts. Rapeseed oil was obtained from Di Luca & Di Luca AB (Stockholm, Sweden). Citric acid and sodium citrate used for buffer preparation, and D_2O were of analytical grade and obtained from Sigma-Aldrich (St. Louis, MO, USA).

2.2. Sample preparation (protein dispersions & emulsions)

The dispersion and emulsion samples are described in terms of overall water/buffer content (% v/v), oil content (% v/v) and protein content (% w/v), where a sample with 15% w/v protein in water/buffer is referred to as 100/0/15 and a sample with 60% v/v water/buffer, 40% v/v oil and 7.5% w/v protein is labelled as 60/40/7.5.

Dispersions of pea protein in water or buffer were prepared with 15% w/v protein. The pH was controlled with a 0.1 M citrate buffer solution with different concentrations of citric acid and sodium citrate to obtain pH values of 3.0, 4.6 and 6.2 [20]. Additionally, a sample with water had

a measured pH of 6.5. The pH values in the buffer solutions and in the dispersions after preparation were verified with pH indicator paper.

Emulsions were prepared with 40, 50 and 60% v/v oil, 60, 50 and 40% v/v water or buffer at the same pH values as for the dispersions, and with a fixed overall protein concentration of 7.5% w/v. The D_2O content in the water was varied between 0 and 100% v/v for the neutron experiments for the purpose of contrast variation.

All samples, including both dispersions and emulsions, were homogenized with a D1000-M5 rotor-stator homogenizer with a 5 × 50 mm flat bottom probe (Benchmark Scientific Inc., Edison, NJ, USA) at maximum speed for 1 min. Samples were used within one week of preparation. Previous work has shown that scattering or droplet size in microscopy images did not change significantly over this period [7,9].

2.3. Spin-Echo small angle neutron scattering (SESANS)

SESANS experiments were performed at the Delft University of Technology. The experiments include measurements of 1) dispersions of protein in water/buffer in pure H_2O, 2) dispersions of protein in water/buffer in pure D_2O, 3) emulsions with different oil fractions and pH in pure H_2O, and 4) emulsions with different oil fractions and pH in 10% D_2O + 90% H_2O. The samples in pure H_2O and D_2O, respectively, were chosen to provide scattering intensity from all components. The last contrast (10% D_2O + 90% H_2O) was chosen to match out most of the scattering signal from the oil and enhance the signal from the protein. The change of isotope was assumed to have no major effect on the protein network structure. Previous SAXS studies of three different isotope mixtures showed identical results [9]. The samples were measured in fused quartz cells with thickness, t, of 2 mm and the measurements were made with a neutron wavelength, λ, of 2.1 Å.

Details about the principles of the technique and the SESANS instrument are described by Rekveldt et al. [21]. In summary, SESANS determines the real-space correlation functions, G(δ), at spin-echo lengths, δ. The spin-echo length represents the real-space correlation distance over which structural inhomogeneities depolarize the neutrons. The polarization, P(δ), is given by

$$P(\delta) = \exp\left(t\lambda^2(G(\delta) - G(0))\right) \quad (1)$$

as described by Bouwman [22]. Unlike conventional small angle scattering techniques, which probe structural information in reciprocal space via the momentum transfer Q, SESANS yields measurements directly in real space. The results are plotted in the form $G(\delta) - G(0) = \ln(P(\delta))/t\lambda^2$ versus δ. The correlations decay with increasing δ from δ=0 to an upper feasible value of δ=20 μm at this wavelength. The observation of saturation indicates that correlations are limited to an upper characteristic size, whereas the presence of a continuous decay indicates that the characteristic lengths of structures are greater than the experimental limit. The data were reduced using custom scripts developed in Delft.

Structural models were fitted to the scattering data using SasView [23]. The fitting procedure, with scattering from fractal systems in terms of interacting proteins and sphere objects in terms of oil droplets, is described in detail in the Supporting Information. Schematics of the model fits for both dispersions and emulsions are presented in Fig. 1. The

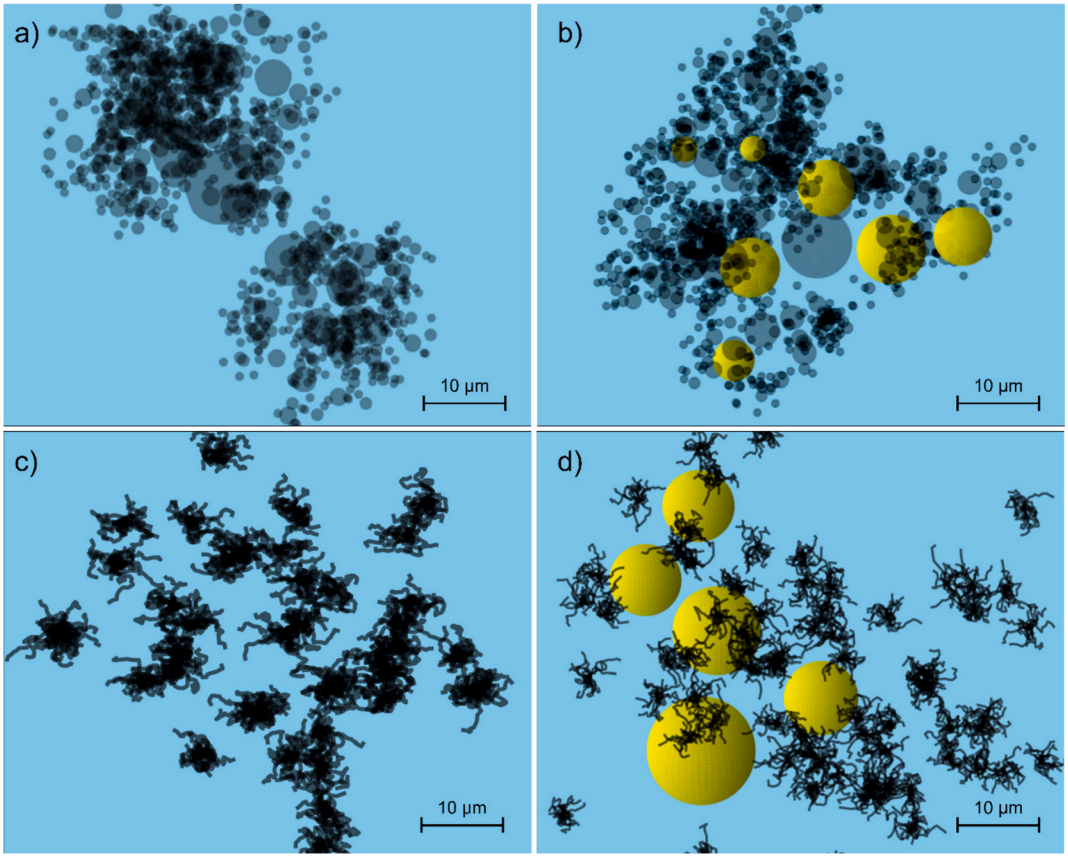

Fig. 1. Schematic diagrams of the a) mass fractal structure used to describe the dispersions in water at neutral pH in Section 3.1, b) mass fractal structure combined with spherical oil droplets used to describe the emulsions prepared with water at neutral pH in Section 3.2, c) structure described by the Guinier-Porod model used to describe the scattering from clusters in the dispersions with a surface fractal in buffer at pH 3.0 and 4.6 described in Section 3.3, d) dispersion described by the Guinier-Porod model combined with spherical oil droplets used for the scattering from emulsions prepared with buffer at pH 3.0 and 4.6 in Section 3.4. Proteins are shown in black with grey representing a hydrated material, oil droplets are in yellow, and the continuous water/buffer phase is in blue. (For interpretation of the references to colour in this figure legend, the reader is referred to the web version of this article.)

model fit parameters are presented in Table S1 in the Supporting Information. Comparison of the parameters between samples are presented in colour plots in Figs. S5 & S6. An additional table of the fitted levels from 10 to 14 μm is provided in Table S2.

2.4. Small angle X-ray scattering (SAXS) & ultra-small angle X-ray scattering (USAXS)

SAXS and USAXS experiments were performed at Uppsala University on the Xeuss 2.0 Q-Xoom instrument (Xenocs, Grenoble, France). The measurements were performed at two sample-to-detector distances of 300 and 2400 mm and the X-ray wavelength was fixed at 1.54 Å. The measurement arrangement is described in more detail in previous work [24]. The resolution for the model fits used 2% for the pinhole SAXS and desmeared USAXS data and a slit length of 0.0015 $Å^{-1}$ for the slit smeared USAXS data. A relaxation factor of 0.3–0.5 was used to desmear the USAXS data. The scale factors in the model fits were allowed to vary 10% due to the uncertainty in thicknesses with the flexible Kapton windows reforming under the viscous samples. The fitting procedure is described in detail in Section 1 in the Supporting Information.

2.5. Small angle neutron scattering (SANS)

SANS experiments were performed at the SANS-1 beamline at the Swiss Spallation Neutron Source (SINQ) [25] at the Paul Scherrer Institute, Switzerland. The data and measurement protocol have been published previously [9]. The analysis and model fitting are extended further in this paper. The fitting procedure is described in detail in Section 1 in the Supporting Information and the instrument resolution used in the model fits was 10% in $\Delta Q/Q$.

3. Results and discussion

The results of the various scattering experiments will be described first for the protein dispersions (Section 3.1) and then the emulsions (Section 3.2), both made with water. Then the effects of different pH will be presented in Section 3.3 and Section 3.4, where the final section discusses the changes in emulsion droplet size and stability that arise from the changes of the protein at specific pH in the presence of buffer salt.

3.1. Protein dispersions: Properties at neutral pH

SESANS was used to investigate the structure of protein dispersed in water. The dispersions contained 15% w/v pea protein in H_2O and D_2O, respectively. The SESANS data were analysed using a fractal model appropriate for large-scale heterogeneous structures (see Fig. 1a). Plots of the data and model fits are shown in Fig. 2. The two different contrasts are fitted to a single model of the structure. This model has previously been used to describe the same gelled protein network system in emulsions on the length scales probed by SANS [9], but are now analysed directly and on larger length scales. The parameters of the fits are summarized in Table S1 in the Supporting Information. The volume fractions of the protein dispersions (fractal model scale factors) were set to 0.14. This factor is calculated as $\varphi_p = V_{pf}(1 - V_{pf})$, where V_{pf} is the total volume fraction of building blocks that in this case consist of hydrated proteins. V_{pf} is obtained by assuming a density of 1.37 g cm^{-3} for the proteins [26] and about 60% hydration (water volume fraction inside the protein building blocks).

A block radius of 38 Å with a log-normal distribution width of 0.5 agrees with that expected for proteins of similar sizes. Pea protein is a mixture of vicilin (146 kDa), convicilin (210–290 kDa) and legumin (300–400 kDa) [8]. Assuming an average weight 150–350 kDa gives a radius 35–47 Å [26]. The fitted fractal dimension was 2.75, indicating a mass fractal network characteristic of porous or highly branched

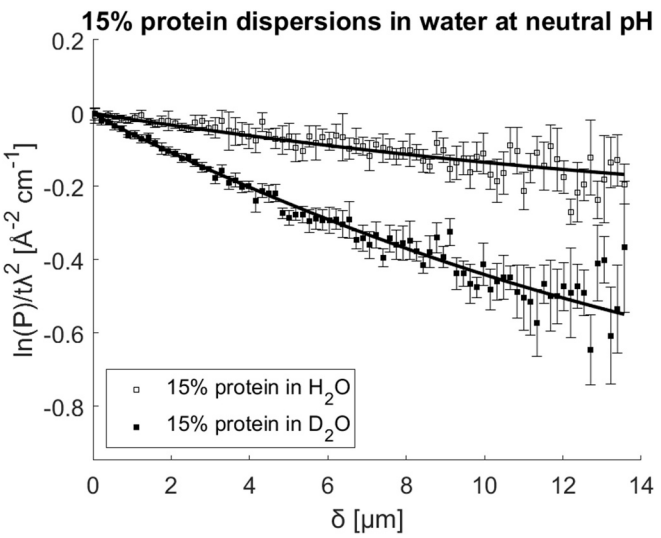

Fig. 2. Results of SESANS measurements for 15% w/v protein dispersions in water with two different contrasts of 100% H_2O (unfilled squares) and 100% D_2O (filled squares) respectively. Continuous lines show the fits to a model of a fractal structure.

polymer networks. The correlation length of 12.7 μm suggests that the structures extend beyond the accessible length scale of the SESANS instrument. This interpretation is supported by the absence of a plateau in the SESANS signal at longer spin-echo lengths, δ, in Fig. 2. This indicates the presence of structures larger or of the same order as the detection limit of 14 μm.

The fitted SLD of the protein blocks was markedly different between the samples with different solvents (H_2O and D_2O). The SLD of the protein blocks in hydrogenated water, ρ_{p+H_2O}, is 0.13×10^{-6} $Å^{-2}$ (solvent SLD, ρ_{H_2O}, is -0.56×10^{-6} $Å^{-2}$) and the SLD of the protein blocks in deuterated water, ρ_{p+D_2O}, is 5.10×10^{-6} $Å^{-2}$ (solvent SLD, ρ_{D_2O}, is 6.35×10^{-6} $Å^{-2}$). Assuming that the SLD is a two-phase volume average with hydration, φ_w, and that the SLD increase of the protein itself due to the hydrogen to deuterium exchange at the labile sites is given by Δ, this can be composed into a system of equations:

$$\rho_{p+H_2O} = (1 - \varphi_w)\rho_{p\ in\ H_2O} + \varphi_w \rho_{H_2O} \quad (2)$$

$$\rho_{p+D_2O} = (1 - \varphi_w)(\rho_{p\ in\ H_2O} + \Delta) + \varphi_w \rho_{D_2O} \quad (3)$$

where $\rho_{p\ in\ H_2O}$ is the SLD of protein equilibrated in H_2O. Solving for φ_w, assuming an exchange correction of $\Delta = 0.56 \times 10^{-6}$ $Å^{-2}$ [27], gives a hydration of 69% *v*/v water inside the protein building blocks and a SLD of protein in H_2O, $\rho_{p\ in\ H_2O}$, as 1.70×10^{-6} $Å^{-2}$. The proton exchange is seen as the dashed black line in Fig. 3. The values for the hydration and protein SLD are well in line with those of amino acids reported by Jacrot [27] and is consistent with the internal solvation of globular or disordered protein networks. This indicates that a substantial amount of water is retained within the protein blocks. The observed SLD due to the hydration within the protein blocks is observed as the black line in Fig. 3, featuring the SLD of the protein blocks as a linear function of D_2O content from the model fits for the protein in non-deuterated (H_2O) and deuterated (D_2O) solvents (unfilled and filled black squares). The blue line in this figure represents the theoretical SLD of the water phase. The average contrast matching point of the protein blocks and the water is found at the intersection between the lines at 35.6% v/v D_2O. The results validate the use of the SESANS technique to determine internal solvation of the protein, which can be used to understand the spatial organization within protein systems.

A simple analysis of the scale factor of the signal strength between 10

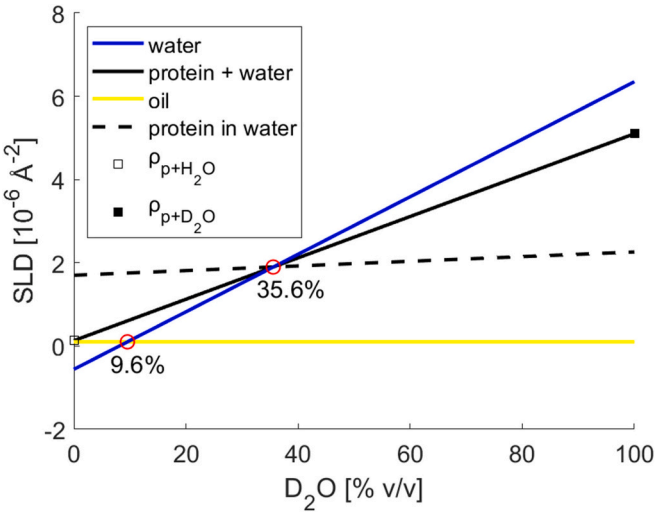

Fig. 3. Change of SLD for various components with D_2O fraction in the aqueous phase for water at neutral pH. The blue line represents the SLD of the pure aqueous phase. The yellow line shows the SLD of oil that does not change with D_2O content. The intersection between these lines is at 9.6% D_2O (red circle) and this value is used for the contrast matching between the oil and the water phase in the experiments. The black solid line is the SLD of the protein blocks in the aqueous phase that changes with D_2O content due to the water content inside the blocks (hydration) as well as exchange of protons between the protein and water. This was calculated based on the model fits in Fig. 2 to the protein in 100% H_2O, ρ_{p+H_2O}, and 100% D_2O, ρ_{p+D_2O}, respectively. The intersection with the SLD of water occurs at 35.6% D_2O (red circle). The dashed black line is the effect only due to the exchange of protons between the protein and water. (For interpretation of the references to colour in this figure legend, the reader is referred to the web version of this article.)

and 14 μm in Fig. 2, described by Andersson et al. [28], gives further clues about the quality of the fits of the protein block SLD. The ratio of the signal strength (0.475 Å^{-2} cm^{-1}/0.170 Å^{-2} cm^{-1}) gives a factor of 2.8, and is not significantly different from the ratio of the square of the SLD differences in the fits which gave a factor of (((1.25 × 10^{-6} Å^{-2})/(0.69 × 10^{-6} Å^{-2}))^2=) 3.3. A table of the signal strengths for all samples are provided in Table S2 in the Supporting Information.

In addition to the SESANS analysis, complementary SAXS and USAXS measurements were performed on the 15% w/v pea protein dispersions in H_2O to probe the structure across a broader range of length scales. Both SAXS and USAXS data sets were well described using the same fractal model applied in the SESANS analysis, with parameters in Table S1 and shown in Fig. S5 in the Supporting Information. The data are plotted in Fig. 4 with the same fractal model of protein block radius 38 Å, fractal dimension 2.75 and correlation length 12.7 μm. Both desmeared and slit-smeared USAXS data are shown. The desmeared data are useful for simple visualization when plotted together with the SAXS data, but the original slit-smeared data were used to evaluate model fits as no information is lost or noise added with a desmearing procedure. The results confirm the presence of protein blocks with the expected size range for globular proteins such as vicilin and legumin, which is better approximated from the SAXS technique investigating smaller structures such as individual protein molecules. The fit to the USAXS data further validates the fractal dimension and the correlation length describing a mass fractal protein network across length scales covered by both X-ray and neutron scattering techniques.

The contrast between the protein and the solvent in the X-ray measurements, driven by electron density differences, was determined as a protein block SLD of 10.6 × 10^{-6} Å^{-2} and with water SLD of 9.41 × 10^{-6} Å^{-2}. The relatively low contrast is not surprising given the high hydration of the protein blocks estimated from the SESANS results. Although it is difficult to determine the correlation length directly from

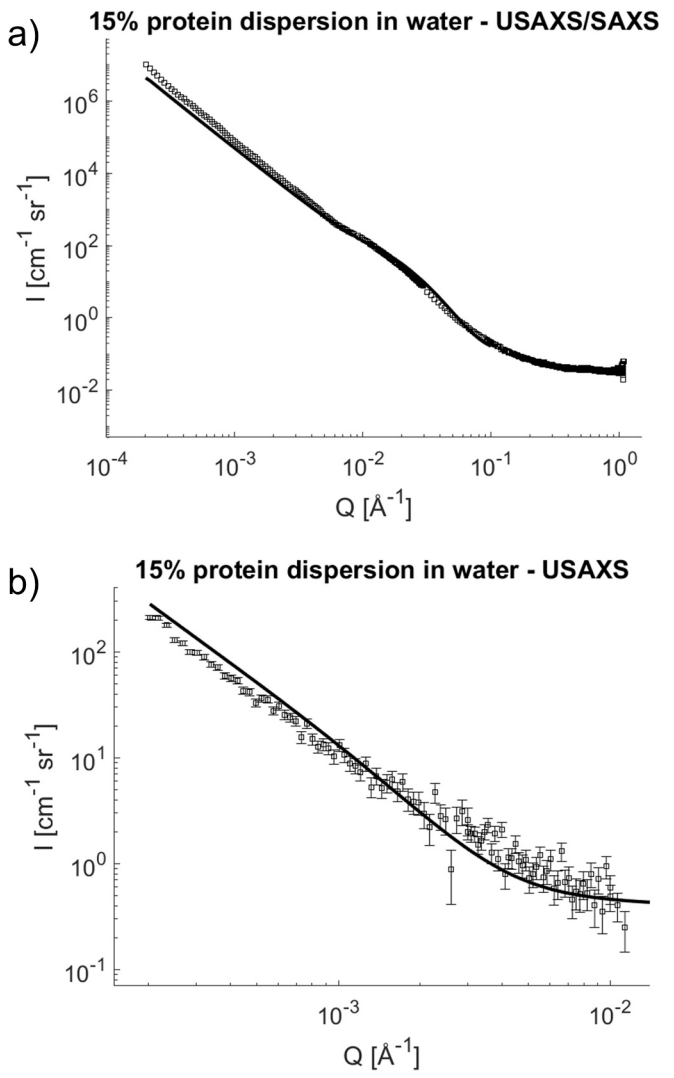

Fig. 4. a) Desmeared USAXS and SAXS data of 15% w/v protein dispersion at neutral pH in water. The techniques cover a total Q range of 2 × 10^{-4} to 1 Å^{-1}. b) Slit smeared USAXS data of the same sample. Model fit parameters of the black lines are presented in Table S1 in the Supporting Information.

SAXS and USAXS, these techniques reinforce the robustness of the fractal description of the protein across multiple length scales obtained from SESANS. The picture of a hierarchical organization of the protein as a porous network is important to understand the role of protein as emulsion stabilizers where oil is added.

3.2. *Emulsions: Changes of droplet size with composition at neutral pH*

These high-protein content emulsions can be thought of as oil droplets dispersed in an aqueous medium consisting of protein dispersed in water. This is sometimes referred to as emulsion-filled gels [29] or fluid emulsion gels [30]. It is relevant to understand the behaviour of protein in water alone in Section 3.1 to be able to discuss the mechanism of stability in emulsions and determine how the oil droplet size vary for different emulsion compositions. SESANS results for emulsions prepared with water of both 100% v/v H_2O and of 10% v/v D_2O + 90% v/v H_2O, respectively, are presented in Fig. 5. The samples with the 10% v/v D_2O fractions are prepared to achieve a SLD of water similar to that of the oil (0.10 × 10^{-6} Å^{-2}), which is seen as the intersection of the blue and yellow SLD lines in Fig. 3. This value is estimated from previous calculations of oil composition and density, compared to SANS experiments with multiple different contrasts [9] and verified with values from the

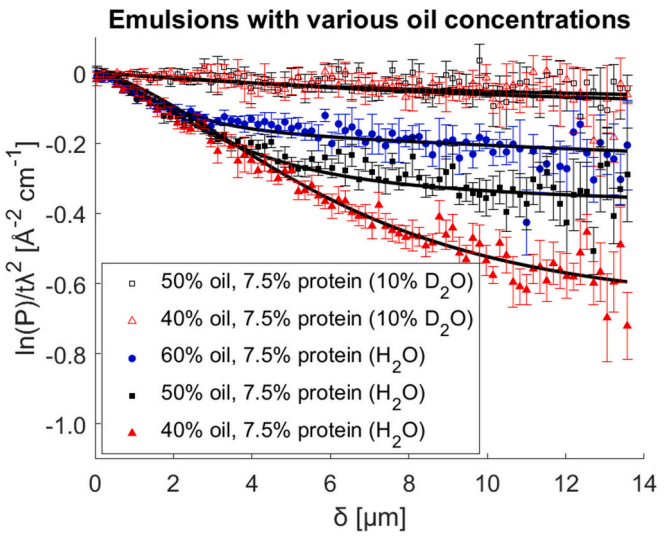

Fig. 5. Results from SESANS of emulsions with 7.5% w/v protein and 60 (blue circles), 50 (black squares) and 40% v/v (red triangles) oil at neutral pH. Data are shown for samples prepared with 100% H_2O (filled symbols) and 10% D_2O + 90% H_2O (unfilled symbols), respectively, where the latter have a much lower scattering power due to the oil/water contrast match condition. Black lines show model fits with parameters in Table S1. (For interpretation of the references to colour in this figure legend, the reader is referred to the web version of this article.)

literature [16]. At this contrast (10% v/v D_2O + 90% v/v H_2O), only contributions to scattering from the proteins are observed. The emulsions in Fig. 5 consist of 40–60% v/v oil and a total of 7.5% w/v protein. Hence, this total protein concentration effectively corresponds to the same concentration in the aqueous phase as for the 15% w/v protein dispersions shown in Fig. 2 and discussed in Section 3.1. The model fits in the figure are calculated as a combination of the scattering from protein dispersed in water, and oil droplets dispersed in this aqueous medium. The model parameters are presented in Table S1 in the Supporting Information. The fractal model with the same parameters as for the protein dispersion in Section 3.1 (protein block radius 38 Å, fractal dimension 2.75 and correlation length 12.7 μm) describes well the protein behaviour in the emulsions. This quantitative fit provides a clear indication that most of the protein in these emulsion samples is present as dispersed material in the aqueous phase. An additional model of polydisperse spheres represents the oil droplets dispersed in this medium with a slightly higher SLD for neutrons than that of pure water (-0.40 to -0.35×10^{-6} Å^{-2} rather than -0.56×10^{-6} Å^{-2} in pure H_2O and 0.22×10^{-6} Å^{-2} rather than 0.13×10^{-6} Å^{-2} in 10% v/v D_2O + 90% v/v H_2O) due to the protein present in this phase.

Considering the emulsions prepared with 100% v/v H_2O, where the scattering signal is the strongest, there are two main features to note. First, the saturation spin-echo length, δ_{sat}, where the curves flatten, is higher for lower oil concentrations. This is reflected in the model fits with parameters in Table S1 in the Supporting Information, where the droplet radii increase as 0.85 μm, 1.5 μm and 2.7 μm for oil concentrations 60, 50 and 40% v/v, respectively.

Secondly, the scattering power or depolarization, seen as the decay in intensity signal, is greater for lower oil concentrations. This can be determined by comparing the scale factors at the highest δ values (from 10 to 14 μm). For instance, the difference in saturation, assuming a flat level, is a factor of (0.563 Å^{-2} cm^{-1}/0.233 Å^{-2} cm^{-1}=) 2.42 for the samples with 40 and 60% v/v oil. This is a consequence of the difference in characteristic length scale directly affecting the scattering power. Comparing the droplet sizes, assuming a radius of 0.85 μm for the sample with 60% v/v oil, would give droplet radii of 1.39 and 2.13 μm for the samples with 50 and 40% v/v oil, respectively. The 8% and 27% deviations from the model fits (1.5 and 2.7 μm), respectively, arise from the polydispersity, where, particularly for the 40% v/v sample, it contains large objects preventing a true plateau to be reached. This can be seen from the tail in the log-normal distribution with a width parameter of 0.5 that is the ratio of the standard deviation of the normal distribution to the median value.

To assess the robustness of the model one can compare samples with multiple contrasts in normal SANS. Such data have been published previously [9], with slightly refined parameters based on the new information about droplet size and fractal correlation length obtained from the SESANS data. The data with model fits and parameters for seven different D_2O/ H_2O fractions are presented in Fig. S3 and Table S1 in the Supporting Information. At the higher D_2O concentrations, close to the water/protein contrast match of 35.6% v/v (see Fig. 3), the majority of the intensity from the protein blocks are hidden. This is observed as the absence of the protein correlation peak around Q of 2.5 $\times 10^{-2}$ Å^{-1}. Such a peak is clearly visible at lower D_2O concentrations closer to the oil/water contrast match conditions. A closer look at the SLD of the protein blocks reveals that they correspond well with the expected values on the black line in Fig. 3. To visualise the good agreement, the values have been added to a plot of SLD in Fig. S2 in the Supporting Information. However, when examining the SLD of the solvent seen by the oil droplets, which consist of both water and protein, these values do not strictly follow the expected linear dependency on the D_2O content at a value between that of the SLD of the protein blocks (solid black lines in Fig. 3 and Fig. S2) and of pure water (blue lines in Fig. 3 and Fig. S2). The values are greater than those expected to achieve a sufficient contrast and upturn at the lowest Q values measured by SANS. The likely explanation for the discrepancy is the presence of denser layers of protein at the droplet interface which alter the contrast between the oil and the water. This is not unreasonable considering the reported interfacial activity of pea proteins [31,32].

The SANS data are primarily useful to understand protein behaviour on smaller length scales than can be derived from SESANS data alone. The data help to validate the size of the protein blocks as well as confirm the hydration of the protein thanks to the many contrasts measured. The results are also useful to validate the SLD of the oil. Combined, the SANS and SESANS results provide information about the protein building block size, the fractal network organization of these and the incorporated oil droplets within the gelled medium. The schematic in Fig. 1b is a good visualization of the emulsion structure.

3.3. *Protein dispersions: Properties in buffer at different pH*

Material behaviour at different pH values is clearly relevant for many emulsion food applications such as in products ranging from mayonnaises, fermented products and vinaigrettes to milk and plant-based milk alternatives, spanning from acidic to neutral pH values. That the pea proteins are behaving differently in dispersions of different pH is easily observed from the SESANS data in Fig. 6, where the signal strength between 10 and 14 μm of the 15% w/v protein dispersion in buffer at pH 4.6 is (0.629 Å^{-2} cm^{-1}/0.170 Å^{-2} cm^{-1}=) 3.7 times greater than the same sample prepared in water at neutral pH. This ratio is (0.297 Å^{-2} cm^{-1}/0.170 Å^{-2} cm^{-1}=) 1.7 for the dispersion in buffer at pH 6.2. For the calculation of the signal strength, the adjustable parameters are the characteristic length scale, the volume fraction and the SLD contrast. The model fits in Fig. 6 are based on a fraction of the protein having the same gelling and fractal system behaviour as at neutral pH. The remaining part of the protein is fitted with the Guinier-Porod model to describe regions of large and denser aggregates of unfolded proteins. This idea arose from observations with confocal microscopy, where large clusters of proteins were observed particularly at acidic pH as opposed to a fine-stranded and homogeneous network at neutral pH [7]. The parameters for the combined fractal and Guinier-Porod models are listed in Table S1 in the Supporting Information. The protein in water at neutral pH, described in Section 3.1, fits well to a

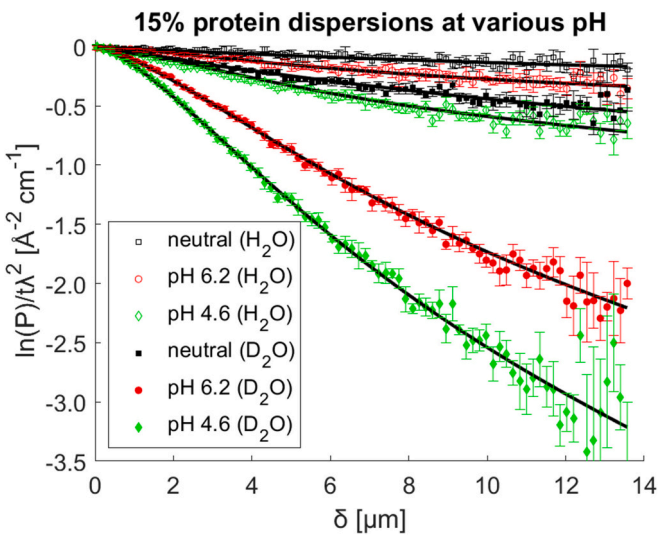

Fig. 6. SESANS data for 15% w/v protein dispersions in water/buffer with two different contrasts of 100% H_2O (unfilled symbols) and 100% D_2O (filled symbols) respectively. Protein in buffer at pH 4.6 (green diamonds) and pH 6.2 (red circles), and in water at neutral pH (black squares). Continuous lines show the model fits with parameters in Table S1 in the Supporting Information. (For interpretation of the references to colour in this figure legend, the reader is referred to the web version of this article.)

single fractal model. The protein in buffer at pH 4.6 can rather be described by the Guinier-Porod model with a radius of gyration of 1.2 μm and a power-law exponent around 3.6. These values are suggesting large clusters of fractal-like or roughened surface. The sample in buffer at pH 6.2 contains protein of both conformations (fractal structure (fractal model) and bigger aggregates with rough surface (Guinier-Porod model)), which is reflected in the model parameter list as a combination of the two protein conformations present at acidic and neutral pH.

To validate the use of these models, additional results from USAXS and SAXS for the dispersions at neutral pH, at pH 6.2 and at pH 3.0 are plotted in Fig. 7 with model parameters in Table S1 in the Supporting Information. The change in configuration of the protein from neutral to acidic pH is mainly observed at the decrease in peak intensity at the broad shoulder around 0.025 $Å^{-1}$. This has been discussed in our previous work [9]. The peak feature is arising due to the size of the protein blocks composing the elements in the fractal network. One possible explanation to the absence of these protein blocks at lower pH is the addition of citrate salt, known to be a kosmotrope, which interact more strongly with the water than with the protein and decrease the solubility of the protein [33]. This effectively forces the unfolded protein into micrometre sized aggregate clusters, where the rough surface is detected with the SESANS technique.

3.4. Emulsions: Changes of droplet size with pH

Following the significant differences of protein behaviour in water/buffer with pH, changes in the rheological behaviour, droplet size and stability of emulsions with pH, are also expected. SESANS results in Fig. 8 show emulsions at pH 3.0, 4.6 and 6.2 in buffer, with the neutral emulsion sample data from Section 3.2 added as a reference. The big differences in scattering power and shape of curves are clearly observed, with the highest scattering power for the sample at pH 3.0 (Table S2, Supporting Information). This suggests that significantly larger structures with higher SLD contrast to the surrounding medium, are present at lower pH. The model fits take the parameters from the protein dispersions and, similarly as in Section 3.2 for emulsions at neutral pH in water, incorporate spheres to account for the added oil droplets. However, the larger protein structures at acidic pH observed in the dispersions are not sufficient to describe the full difference in scattering power among the samples. The signal strength between 10 and 14 μm for the emulsion in buffer at pH 3.0 is (1.061 $Å^{-2}$ cm^{-1}/0.345 $Å^{-2}$ cm^{-1}=) 3.1 times greater than the same sample prepared in water at neutral pH. The signal strength for the protein emulsions in buffer at pH 4.6 and 6.2, respectively, are (0.798 $Å^{-2}$ cm^{-1}/0.345 $Å^{-2}$ cm^{-1}=) 2.3 and (0.509 $Å^{-2}$ cm^{-1}/0.345 $Å^{-2}$ cm^{-1}=) 1.5 times greater than the same sample prepared in water at neutral pH. Therefore, it is apparent that also the droplet size is increasing with decreasing pH.

The trend of increasing droplet radii with decreasing pH is clear and

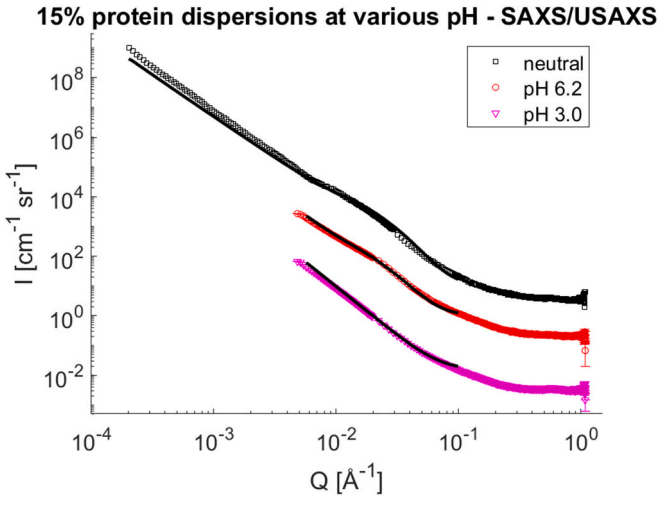

Fig. 7. a) Desmeared USAXS and SAXS data for 15% w/v protein dispersions at neutral pH in water (black spheres), and at pH 6.2 (red circles) and pH 3.0 (purple triangles) in buffer. The techniques cover a total Q range of 2×10^{-4} to 1 $Å^{-1}$. Model fit parameters of the black lines are presented in Table S1 in the Supporting Information. Data for the sample at pH 3.0 is on an absolute scale, other samples are shifted by factors of 100 and 1000 for clarification. (For interpretation of the references to colour in this figure legend, the reader is referred to the web version of this article.)

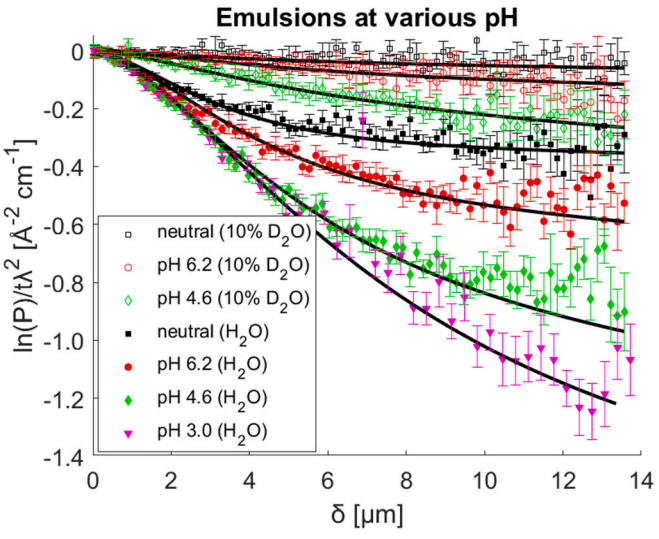

Fig. 8. SESANS results for emulsions with 7.5% w/v protein and 50% v/v oil at neutral pH in water (black squares), at pH 6.2 in buffer (red circles), at pH 4.6 in buffer (green diamonds) and at pH 3.0 in buffer (purple triangles). Data are shown for samples prepared with 100% H_2O (filled symbols) and 10% D_2O + 90% H_2O (unfilled symbols). Continuous lines show model fits with parameters in Table S1 in the Supporting Information. (For interpretation of the references to colour in this figure legend, the reader is referred to the web version of this article.)

the radii span from 1.5 μm for emulsions at neutral pH in water to 1.7, 2.2 and 3.0 μm at pH 6.2, 4.6 and 3.0 in buffer. These values are slightly smaller than deduced from previous microscopy studies [7,9] but within the correct order of magnitude. The slight disagreement could be due to changes of protein configuration from pure dispersions in water/buffer compared to emulsions with the addition of oil. The model fits in the present paper assume that the parameters to describe the protein are the same for the emulsions as for the protein dispersions. However, it is likely that 1) the configuration of the protein, that it is surface-active, will change conformation or assembly on binding to the oil interface, and 2) the overall size of the protein network and the oil droplets would match closely in size as the protein is located in the surrounding space between droplets. This should be noted in the extraction of the exact values of the fit parameters for the droplet and overall protein sizes. However, it is clear that there is a large difference in size of both protein structures and oil droplet sizes with pH as the difference in scattering power cannot be explained by simply one of them alone. It is also likely that the hydration of the protein is very different in the presence of buffer salt, where the high content of water present inside the protein blocks in water at neutral pH is not present to the same extent at lower pH due to the preferable binding to the buffer salt rather than to the proteins.

To validate the quality of the fits and motivate the use of these parameters, it is useful to compare the SESANS results to those obtained from SAXS, USAXS and SANS. These techniques provide multiple additional contrasts and information of smaller length scales. Although there are many parameters for the models for this complex multi component system, measurements with several different contrasts using techniques sensitive to a wide range of length scales allows them to be identified clearly. The evidence for network formation that is crucial for stability is clear. Fig. S4 in the Supporting Information, with data published in [9], shows SANS data for emulsions (50% v/v oil, 7.5% w/v protein) with water at neutral pH and with buffer at pH 6.2, 4.6 and 3.0. The main differences are observed, as for the dispersion samples, near the broad shoulder around $Q = 0.025$ Å^{-1}. This feature disappears at the lower pH values due to the transition of proteins from small individual hydrated building blocks of proteins in the fractal network at neutral pH to aggregates of unfolded proteins at pH 3.0. The model parameters to the fits are presented in Table S1 in the Supporting Information.

Fig. 9 shows USAXS and SAXS data for emulsions (50% v/v oil, 7.5% w/v protein) with water at neutral pH and with buffer at pH 6.2, 4.6 and 3.0. The USAXS results for all samples are similar in many ways, as they are dominated by surface scattering according to the Porod law without a Guinier region which would enable direct determination of the droplet size. The differences in the SAXS data around the broad peak show the same trend as discussed previously (intensity decrease for more acidic pH) for dispersions and emulsions studied by both SANS and SAXS. The model parameters are listed in Table S1 and shown in Fig. S6 in the Supporting Information.

The two main take-away messages from these results are how the droplet radii change with oil concentration and pH. There are clear relationships of decreasing radii with 1) higher oil fractions and 2) towards higher pH. This is visualized in Fig. 10 and corresponds with the confocal microscopy results presented previously [9]. However, unlike microscopy, SESANS investigates a bulk sample with many droplets, providing averaged droplet radii and correlation lengths. This gives systematic results for different compositions and pH that are not easily quantifiable with microscopy images concerning only limited parts of a sample. The probable explanation for the trend with pH is that the proteins aggregate more at low pH rather than remaining as small hydrated building blocks that form big fractal structures at neutral pH. To confirm this explanation, a series of contrasts for acidic pH would be useful to investigate, particularly in the USANS region, to identify whether the hydration is less at low pH. Despite the difference in protein structure and droplet size at different pH, the samples show a similar range of stable compositions [10]. The viscosity of the emulsions at lower pH, however, is higher (Fig. S7a). The elastic and viscous moduli (Fig. S7b) are comparable for the samples except for the sample at pH 3.0 that shows stronger interactions due to the extensive protein unfolding and aggregation. The formation of a fractal branched structure at neutral pH enhance the appearance of a fine-stranded network rather than big aggregated clusters as seen in microscopy images of the emulsions [7,9].

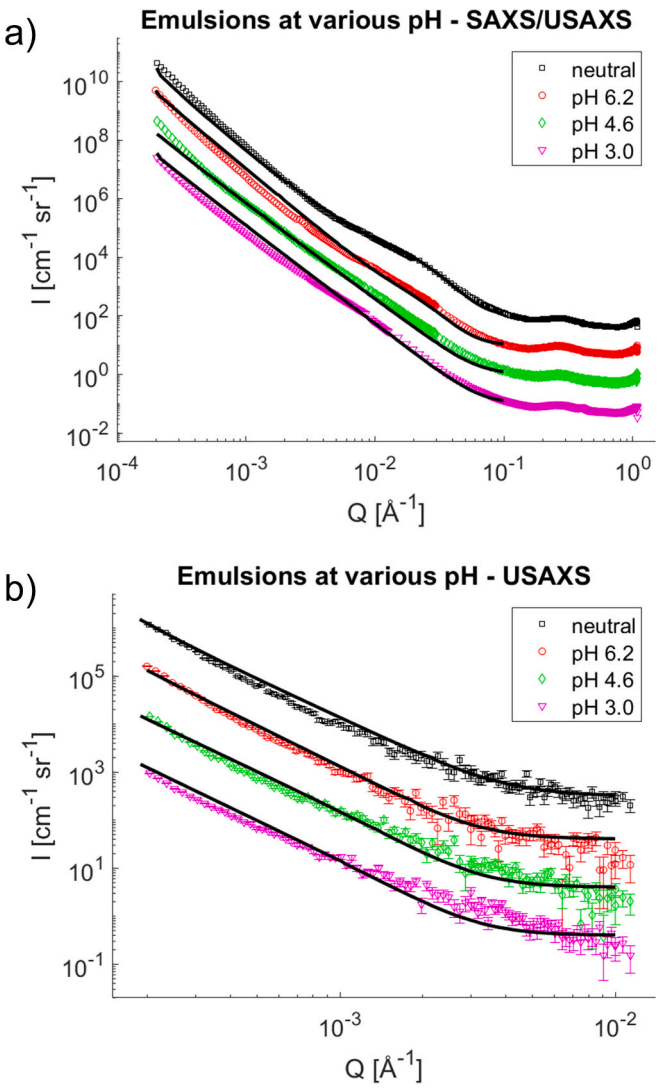

Fig. 9. a) Desmeared USAXS and SAXS data for emulsions with 50% v/v oil and 7.5% w/v protein at neutral pH in water (black spheres), and at pH 6.2 (red circles), pH 4.6 (green diamonds) and pH 3.0 (purple triangles) in buffer. The techniques cover a total Q range of 2×10^{-4} to 1 Å^{-1}. b) Slit smeared USAXS data for the same samples. Model fit parameters of the black lines are presented in Table S1 in the Supporting Information. Data for the sample at pH 3.0 is on an absolute scale, other samples are shifted by factors of 10 for clarification. (For interpretation of the references to colour in this figure legend, the reader is referred to the web version of this article.)

4. Conclusions

This study has highlighted the use of spin-echo SANS for dispersions and emulsions with multiple components (protein networks and oil droplets) of length scales from tens of nanometres to several micrometres. The decay in the SESANS signal for all length scales investigated that is seen for the protein dispersions clarifies the behaviour as a gelled protein network. It is interesting from a physics point of view, as this concludes that there is a fractal system from nanometre sized protein

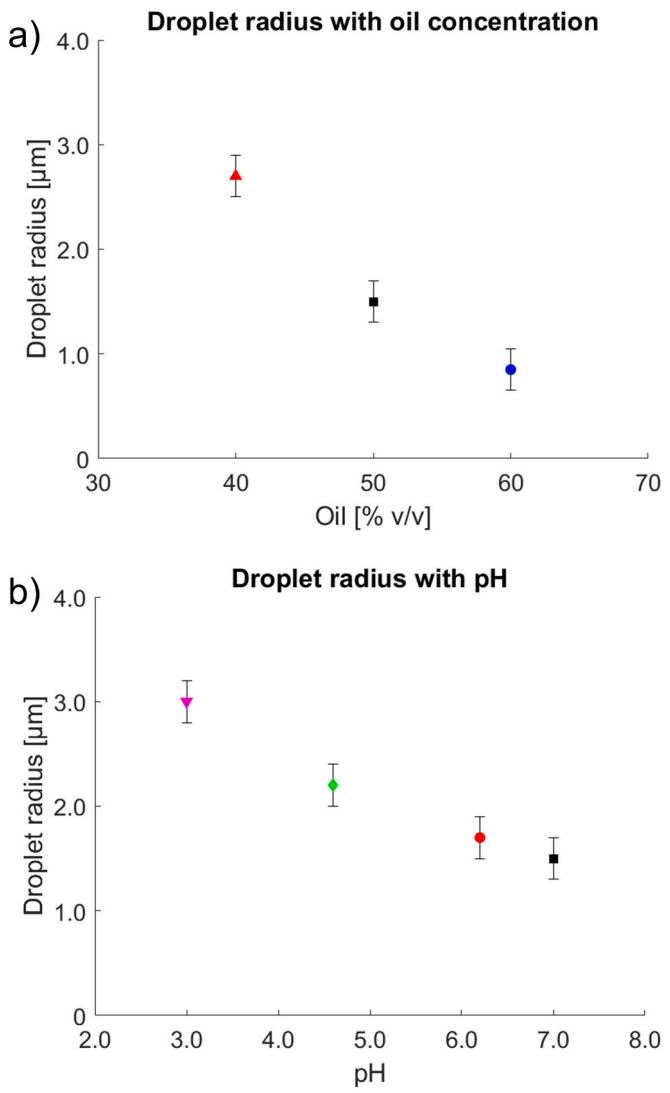

Fig. 10. a) Droplet radius of emulsions with 40–60% v/v oil and 7.5% w/v protein at neutral pH obtained from model fits in Fig. 5 and listed in Table S1 in the Supporting Information. The droplet radius decreases with oil fraction. b) Droplet radius of emulsions with 40% v/v oil and 7.5% w/v protein at pH 3.0 to neutral obtained from model fits in Fig. 8 and listed in Table S1 in the Supporting Information. The droplet radius decreases with pH.

blocks to micrometre sized networks formed. Further to a previous SAXS study of individual proteins [34], the present results provide new knowledge about hydration on larger length scales, which is relevant to overall stability. This finding confirms previous ideas of yield stress being essential for emulsion stability [7]. However, the previous ambiguity of whether the gelation occurrs from jamming of droplets or from interacting proteins has now been resolved. Although pea protein has been reported to be surface active, the stability mechanisms of gelling and viscosity increase of the bulk phase are important for properties where particularly creaminess and fat-mimicking structures can be obtained without saturated fats. Although emulsions with a droplet size of a few micrometres and oil concentrations of the order 50% create a substantial amount of surface area, the stability mechanism of these emulsions cannot simply be described as a pure Pickering type system [5]. Required protein concentrations of the order 5–10% emphasizes that additional protein in the bulk phase is crucial for stability. This could also be relevant for other systems derived from plant-based proteins, as those are likely to interact in similar ways and create emulsion gelled systems at high protein concentrations. Dickinson's review [35] of emulsion gels provides some insights about the rheological properties of other types of emulsion gels, where particularly the stabilization mechanism as physical molecular crosslinks or chemical covalent bonds, depending on the processing made by heating, acidification or enzyme addition, affects the rheology of the emulsion gels. Further, de Carvalho et al. [36] discuss the potential of gelled emulsions to replace saturated fats and the possible advantage of combining plant proteins with polysaccharides as structuring agents. This has been used not only for pea proteins, but also, for example, for soy, quinoa and zein proteins combined with materials such as chitosan, inulin and carrageenan. It is thus not only pea proteins that show this behaviour, which is promising from the perspective to include other plant proteins and generalize the finding from this study. It can also open up ways to use SESANS to study similar complex multi-component materials and perform both fitting of physical models as well as draw more simple conclusions of sizes and structures from scattering power and initial gradients.

Regarding droplet sizes of emulsions, a higher oil fraction gives an effective higher concentration of protein in the aqueous phase (the total protein concentration in the overall emulsions being equal), which strengthen the gelation and hence the stability, preventing droplet coalescence. The larger droplet sizes in emulsions at lower pH can be explained by similar reasoning, where the reduced amount of protein present in the form of a fractal gelling network is not sufficient to keep the good stability and small droplet sizes. The amount of protein that is present as small blocks and aggregated clusters, respectively, could be determined from model fits of the real systems at different pH in SESANS and validated with previous knowledge and complementary techniques (SANS, SAXS and USAXS) confirming the protein block size, hydration and SLD of the different components (protein, water/buffer and oil). A protein hydration close to 70% at neutral pH and protein block size of 38 Å was not observed to the same extent at lower pH in the presence of buffer salt. Additionally, for a system with less previous knowledge about the sample, droplet sizes, SLD contrasts and volume fractions could also be obtained directly from scales of scattering power. It is interesting to note that the different materials in the natural pea protein are enough for both stabilizing the emulsion and to act as gelling agents, hence addition of multiple different materials is not needed. It is also worth mentioning that the gelation occurs without enzyme, heat, acidification, addition of ions, or other treatment of the protein. This makes the plant a particularly interesting candidate to use more frequently in applications.

This study has demonstrated the use of SESANS with contrast matching as a non-invasive technique to study these turbid samples which cannot be studied with other techniques in such a quantitative way. The data interpretation is relatively easy compared to other conventional scattering techniques (SANS, SAXS and USAXS), even for more complex systems consisting of a mixture of protein species and polydisperse droplet sizes.

CRediT authorship contribution statement

Eleonora Olsmats: Writing – review & editing, Writing – original draft, Visualization, Investigation, Formal analysis, Data curation, Conceptualization. **Adrian R. Rennie:** Writing – review & editing, Supervision, Funding acquisition, Conceptualization. **Jeroen Plomp:** Writing – review & editing, Methodology. **Michel Thijs:** Writing – review & editing, Methodology. **Coen Fransen:** Writing – review & editing, Methodology. **Chris Duif:** Writing – review & editing, Methodology. **Wim Bouwman:** Writing – review & editing, Supervision, Methodology, Conceptualization.

Funding

This work was supported by the European Union's Horizon 2020 research and innovation programme under the Marie Skłodowska Curie PICKFOOD project grant number 956248.

Declaration of competing interest

The authors declare that they have no known competing financial interests or personal relationships that could have appeared to influence the work reported in this paper.

Acknowledgements

The authors thank the Delft University of Technology for beamtime on the SESANS instrument. The authors acknowledge the Department of Medicinal Chemistry at Uppsala University for access to the USAXS/SAXS instrument. The authors thank the Swiss Spallation Neutron Source at the Paul Scherrer Institute for the SANS beamtime at SANS-1. This work benefited from the use of the SasView application, originally developed under NSF award DMR-0520547. SasView contains code developed with funding from the European Union's Horizon 2020 research and innovation programme under the SINE2020 project, grant agreement No 654000.

Appendix A. Supplementary data

Supplementary data to this article can be found online at https://doi.org/10.1016/j.jcis.2026.140071.

Data availability

Data for this article, including SESANS, SANS, USAXS and SAXS data sets are available at Zenodo at https://doi.org/10.5281/zenodo.17250750.

SESANS, SANS, USAXS & SAXS data sets (Original data) (Zenodo)

References

[1] C. Albert, M. Beladjine, N. Tsapis, E. Fattal, F. Agnely, N. Huang, Pickering emulsions: preparation processes, key parameters governing their properties and potential for pharmaceutical applications, J. Control. Release 309 (2019) 302–332.
[2] C.C. Berton-Carabin, K. Schroën, Pickering emulsions for food applications: background, trends, and challenges, Annu. Rev. Food Sci. Technol. 6 (2015) 263–297.
[3] F. Goodarzi, S. Zendehboudi, A comprehensive review on emulsions and emulsion stability in chemical and energy industries, Can. J. Chem. Eng. 97 (1) (2018) 281–309.
[4] E.W. Grünewald, R.M. Dalgliesh, S.R. Parnell, W.G. Bouwman, G.N. Smith, Ripening of nonaqueous emulsions of n-Decane in dimethyl sulfoxide observed by time-resolved spin-echo small-angle neutron scattering (SESANS), Langmuir 41 (21) (2025) 12883–12889.
[5] B.P. Binks, Particles as surfactants - similarities and differences, Curr. Opin. Colloid Interface Sci. 7 (1–2) (2002) 21–41.
[6] D.J. McClements, Protein-stabilized emulsions, Curr. Opin. Colloid Interface Sci. 9 (5) (2004) 305–313.
[7] E. Olsmats, A.R. Rennie, D. Bonn, What makes oil-in-water emulsions with pea protein stable? The role of excess protein in network formation and yield stress development, Soft Matter 21 (2025) 3757–3767.
[8] E. Olsmats, A.R. Rennie, Pea protein [Pisum sativum] as stabilizer for oil/water emulsions, Adv. Colloid Interface Sci. 326 (2024) 103123.
[9] E. Olsmats, R.P. Ravindranathan, K.D. Knudsen, J. Kohlbrecher, D. Bonn, A. R. Rennie, Emulsions stabilized by pea protein – hydration and protein distribution, Food Hydrocoll. 162 (2025) 110989.
[10] E. Olsmats, A.R. Rennie, Understanding stabilization of oil-in-water emulsions with pea protein—studies of structure and properties, Langmuir 40 (26) (2024) 13386–13396.
[11] V.F. Sears, Neutron scattering lengths and cross sections, Neutron News 3 (3) (1992) 26–37.
[12] R. Li, J. Lamolinairie, L. Chiappisi, M. Corredig, A time-resolved investigation at multiple-length scales of the structure of liquid foam stabilized by albumins from pea, J. Colloid Interface Sci 678 (Part B) (2025) 1049–1060.
[13] R.H. Tromp, W.G. Bouwman, A novel application of neutron scattering on dairy products, Food Hydrocoll. 21 (2) (2007) 154–158.
[14] L.F. van Heijkamp, I.M. de Schepper, M. Strobl, R.H. Tromp, J.R. Heringa, W. G. Bouwman, Milk gelation studied with small angle neutron scattering techniques and Monte Carlo simulations, J. Phys. Chem. A 114 (7) (2010) 2412–2426.
[15] A. Feichtinger, A. Jarray, W.G. Bouwman, C.P. Duif, M.C. Valverde-Ayllon, K. Heerkens, R. Rooijakkers, J. Landman, E. Scholten, Biopolymer-based capillary suspensions: influence of particle properties on network formation, Food Hydrocoll. 163 (2025) 111061.
[16] A. Bot, F.P. Duval, W.G. Bouwman, Effect of processing on droplet cluster structure in emulsion gels, Food Hydrocoll. 21 (5–6) (2007) 844–854.
[17] A. Bot, F.P. Duval, C.P. Duif, W.G. Bouwman, Probing the droplet cluster structure in acidified temperature-cycled o/ w emulsion gels by means of SESANS, Int. J. Food Sci. Technol. 42 (6) (2007) 746–752.
[18] M. Nieuwland, W.G. Bouwman, L. Pouvreau, A.H. Martin, H.H.J. de Jongh, Relating water holding of ovalbumin gels to aggregate structure, Food Hydrocoll. 52 (2016) 87–94.
[19] T. Heiden-Hecht, B. Wu, K. Schwärzer, S. Förster, J. Kohlbrecher, O. Holderer, H. Frielinghaus, New insights into protein stabilized emulsions captured via neutron and X-ray scattering: an approach with β-lactoglobulin at triacylglyceride-oil/water interfaces, J. Colloid Interface Sci. 655 (2024) 319–326.
[20] G. Gomori, Preparation of buffers for use in enzyme studies, Methods Enzymol. 1 (1955) 138–146.
[21] M.T. Rekveldt, J. Plomp, W.G. Bouwman, W.H. Kraan, S. Grigoriev, M. Blaauw, Spin-echo small angle neutron scattering in Delft, Rev. Sci. Instrum. 76 (2005) 033901.
[22] W.G. Bouwman, Spin-echo small-angle neutron scattering for multiscale structure analysis of food materials, Food Struct. 30 (2021) 100235.
[23] SasView [Online]. Available, http://www.sasview.org. Accessed 17 04 2024.
[24] E. Olsmats, A.R. Rennie, From dairy to plant products: understanding their structural fingerprints with X-rays, Npj Sci. Food 9 (2025) 109.
[25] J. Kohlbrecher, W. Wagner, The new SANS instrument at the Swiss spallation source SINQ, J. Appl. Cryst. 33 (2000) 804–806.
[26] H.P. Erickson, Size and shape of protein molecules at the nanometer level determined by sedimentation, gel filtration, and electron microscopy, Biological Procedures Online 11 (1) (2009) 32–51.
[27] B. Jacrot, The study of biological structures by neutron scattering from solution, Rep. Prog. Phys. 39 (10) (1976) 911–953.
[28] R. Andersson, L.F. van Heijkamp, I.M. de Schepper, W.G. Bouwman, Analysis of spin-echo small-angle neutron scattering measurements, J. Appl. Cryst. 41 (2008) 868–885.
[29] T. Farjami, A. Madadlou, An overview on preparation of emulsion-filled gels and emulsion particulate gels, Trends Food Sci. Technol. 86 (2019) 85–94.
[30] D. Lin, A.L. Kelly, S. Miao, Preparation, structure-property relationships and applications of different emulsion gels: bulk emulsion gels, emulsion gel particles, and fluid emulsion gels, Trends Food Sci. Technol. 102 (2020) 123–137.
[31] C. Amine, J. Dreher, T. Helgason, T. Tadros, Investigation of emulsifying properties and emulsion stability of plant and milk proteins using interfacial tension and interfacial elasticity, Food Hydrocoll. 39 (2014) 180–186.
[32] L. Chang, Y. Lan, B. Chen, J. Rao, Interfacial, and emulsifying properties nexus of green pea protein fractions: impact of pH and salt, Food Hydrocoll. 140 (2023) 108652.
[33] A.N. Mapile, E. Svensson Grape, C.K. Brozek, Solvation of nanoscale materials, Chem. Mater. 36 (19) (2024) 9075–9088.
[34] R. Li, D. Neofytos, J.J.K. Kirkensgaard, A. Pal, J. Skov Pedersen, M. Corredig, In-depth exploration of the structure of pea albumin, its fractions and their heating and foaming properties, J. Colloid Interface Sci. 692 (2025) 137507.
[35] E. Dickinson, Emulsion gels: the structuring of soft solids with protein-stabilized oil droplets, Food Hydrocoll. 28 (1) (2012) 224–241.
[36] M.D. de Carvalho, Â.L. Fazani Cavallieri, A.C. Kawazoe Sato, Plant proteins in structuring gelled emulsions for saturated fat substitutes: challenges and opportunities, Food Res. Int. 202 (2025) 115753.